Chapter 7

Bistatic radar scatterometers for studying vegetation scattering response and its parameter retrieval: A machine-learning study

7.1 Introduction

Bistatic radar signatures derived from vegetation, agriculture crops, forest and soil have emerged as a new area in the field of microwave remote sensing with the enormous potential of monitoring/retrieving vegetation and geophysical parameters of various land covers and soil moisture. In the recent interest, scattering geometry of bistatic radar system where transmitter and receiver are separated spatially and could be located on the ground or low/high altitude onboard spacecraft or a combination of built-in space transmitter with ground locating receiver is also possible [118]. The development of the bistatic system with the various combination of separated transmission and receiving antennas with specular

and off-specular angular geometry led to the advancement in scattering phenomena that might be used in land cover target detection, vegetation monitoring/vegetation growth parameter retrieval and Earth observation [126, 177, 178].

Due to the capability for variability in the geometry of the bistatic system configuration, it has various advantages over the backscattering configuration. In the bistatic system, transmission and receiver are physically separated from each other that will help in providing multi-dimensional information of the target and will be helpful to enhance target radar cross-section due to its geometrical effect [115]. A very few numbers of space-borne bistatic configuration satellites are available for Earth observation. For instance, TanDEM-X (an extension of TerraSAR-X mission) is the first space-borne bistatic radar in orbit to produce a global digital elevation model [34, 134]. However, an application of Global Navigation Satellite System reflectometry (GNSS-R) data over bistatic configuration was firstly used for retrieval of vegetation parameters and land geophysical parameters detailed in [133, 179, 180]. Direct and reflected signal GNSS-R has been studied by specially designed GNSS receiver from the ground and airborne system under bistatic configuration for the larger-scale application by [157, 158, 181–184]. Investigating the interaction of microwave with different media has a wide range of application in the field of remote sensing, communication technology and plasma physics [185–192].

A significant number of theoretical studies based on microwave bistatic scattering mechanisms were aimed at finding optimized bistatic system parameters in terms of frequency, incidence angle and polarization for the different targets while numerous experimental set up of bistatic system has been built for the investigation of agriculture field, forest and soil [140, 193–195]. From a theoretical viewpoint, bistatic models were divided into two groups incoherent models based on vector radiative transfer model which provides only amplitude information and coherent model based on the coherent sum of the complex scattered field which provides both amplitude and phase information [115, 119, 132, 196–

198]. Numerous efforts have been made on microwave bistatic scattering model based on distorted born approximation (DBA) or radiative transfer (RT) theory by [115],[199], and [144] embedded with the characteristics of an antenna and physical property of vegetation/soil [196]. As a matter of fact, according to few popular bistatic scattering models for vegetation and soil which approximates the expression of bistatic scattering intensity into the summation of the coherent and incoherent component in which coherent component is dominated by soil characteristic beneath vegetation and incoherent component is introduced by characteristics of vegetation growth parameter. The component of scattered intensity is also dependent on frequency, polarization and incidence angle for better model calibration and validation. In [115], the Michigan microwave canopy scattering model [MIMICS] was developed in bistatic configuration hence called Bi-MIMICS model. Bi-MIMICS model uses first-order radiative transfer theory which analyzes the contribution of microwave interaction with ground and vegetation canopy to the total scattering from multiple viewpoints in terms of polarization, incidence angle, scattering angle, and azimuth angle. The simulation result shows that the bistatic scattering coefficient is more sensitive to forest biomass in comparison with monostatic. The first order Michigan Microwave Canopy Scattering (MIMICS) model on wheat and soybean at L and C bands was also used to investigate the influence of crop height, leaf size and vegetation water content and soil beneath vegetation on total scattering echoes described in [117]. Results of the simulation show that retrieval of vegetation parameter and soil moisture beneath vegetation was preferred at higher frequency (C band) and at a lower frequency (X band), respectively. A fully polarimetric electromagnetic Tor Vergata model (TOV) was developed at Tor Vergata university used to analyze specular attenuation of incoherent scattering (scattering due to soil underneath) provided by vegetation and the results show that vegetation water content and fresh biomass shows appreciable sensitivity in comparison with monostatic configuration [116, 200]. Further, this well-established TOV model was extended for

bistatic configuration in off specular direction to investigate the potential of bistatic radar for vegetation parameter retrieval by [118]. These models were used to visualize the response of real measurement situations. Therefore, there is a need to analyze experimental results for the bistatic system configuration of different vegetation targets to check the reliability of theoretical developed model. Along with the understanding of the microwave interaction with vegetation, forest and soil, the mathematical expression of the bistatic scattering coefficient which relates the amount of radiation scattered from any target in particular direction involves complex mathematical expression. To overcome the complexity of the model, nowadays the robust machine learning algorithms have been widely used in the field of remotely sensed data for agriculture for classification and regression purposes [201–206].

This Chapter presents an experimental set up of interaction of microwave frequencies with rice crop for bi-spec configuration and retrieval of vegetation parameters of paddy crop by keeping following goals in mind: 1) to explore new measurement technique in bistatic direction for crop monitoring and crop vegetation parameter retrieval; 2) to develop an understanding of scattering mechanism of indigenously design ground-based scatterometer system with bi-spec configuration 3) to find the optimum parameter of the developed system in terms of frequency, polarization and specular angle for vegetation parameter retrieval; 4) to deliver validation/testing datasets over trained machine learning algorithms in the context of vegetation parameter retrieval in remote sensing and; 5) to develop a methodology as a reference for future advancement in bistatic radar system and field study.

7.2 Methodology

7.2.1 Ground-based measurement description

In order to test the sensitivity of the bi-spec scatterometer system over the vegetated field, an experiment was conducted on specially prepared outdoor paddy crop bed beside the Department of Physics, IIT (BHU), Varanasi. The study area is situated in Uttar Pradesh, India, and its location is described by latitude $25^{\circ}15^{'}32^{''}$ N and longitude $82^{\circ}59^{'}34^{''}$ E. On 212, day of the year (DoY) 2018, the pre-germinated rice seedlings were transferred from seedbed and transplanted to leveled outdoor wet field of an area 10 m×10 m with row and column spacing of 0.15 m and 0.20 m, respectively. Management of Water, nutrients and effective method to control harmful insects, disease and weeds were taken care of to maintain crop health. Measurements were taken for different growth stages of paddy crop from 232, DoY 2018 till 312, DoY 2018. Each measurement for bi-spec scattering response and vegetation growth parameters (i.e., LAI, PH, FBm and VWC) were taken on the same day and repeated at the interval of 10 days. The experimental arrangements of the bistatic scatterometer system is shown in Figure 4.1 of Chapter 4. For each bi-spec scattering measurement, soil moisture was kept constant by irrigating paddy crops up to $0.05m$ from soil surface till the maturity stage (i.e.. 302, DoY 2018) attained to meet the seasonal condition. The average of five vegetation sample at five different locations from paddy crop bed was used to compute LAI, PH, FBm and VWC on the same date of the bi- scatterometer measurement. LAI-2200C plant canopy analyzer (LI-COR, Inc.) and meter scale were used for the measurements of LAI and PH, respectively. The destructive sampling method was used to compute FBm and VWC of paddy crop. In this method, FBm were calculated by the averaging weight of five fresh paddy cluster sample from five different locations multiplied by paddy cluster density, i.e., the number of paddy clusters per square meter. Further, the average dry weight of the same five paddy clusters was

calculated by drying it in an oven at 60°C for 72 hours for the calculation of VWC. The value FBm and VWC of paddy clusters were computed by Eqs. 7.1 and 7.2.

$$FBm = (\frac{1}{5}\sum_{i=0}^{5} W_{Fresh\ cluster_i})\eta \tag{7.1}$$

$$VWC = [\frac{1}{5}\sum_{i=0}^{5} (W_{Fresh\ cluster_i} - W_{Dry\ cluster_i})]\eta \tag{7.2}$$

Where $W_{Fresh\ cluster}$ is the weight of fresh paddy clusters and $W_{Dry\ cluster}$ is the weight of dry paddy clusters, η is cluster density per square meter.

7.2.2 Bistatic specular (Bi-spec) scatterometer system

Table 7.1 Specification of the bi-spec scatterometer system.

Parameters	Specifications	
Bands	X band (8.2-12.4 GHz)	C band (4.6-7.05 GHz)
Frequency used	10 GHz	6 GHz
Antenna Gain	20 dB	20 dB
Beam-width		
E-Plane (°)	16.5°	16.9°
H-Plane (°)	16.1°	14.3°
Waveguide size	WR-90	WR-159
RF generator	High power continuous wave generator (PSG), (E8257D, 10 MHz–20 GHz)	
Power meter	The power meter of the EPM-P series (E4416A, 9 kHz to 110 GHz)	
Power sensor	Average and peak power sensor (E9327A, 50 MHz–18 GHz)	
Polarization modes	Horizontal transmit–horizontal receive (HH) Vertical transmit–vertical receive (VV)	
Platform height	3 meter	
Incident angle	20° - 60°	

A pair of WR-90 waveguide standard gain horn antenna operating from 8.2 GHz to 12.4 GHz for X band and a pair of WR-159 waveguide standard gain horn antenna operating from 4.9 GHz to 7.05 GHz for C band with a nominal 20 dB gain from Pasternak

enterprises were used for the study. 10 GHz at X band and 6 GHz at C band were used for bistatic system configuration. Horizontal and vertical beam-width of X and C band were (16.1°, 16.5°), (14.3°, 16.9°), respectively. A pair of moving standard gain horn antenna (transmitting and receiving) was mounted on a horizontal track, 3 meters above the paddy crop bed for the measurement of microwave scattering at a specular angle of incidence varying from 20° to 60°. Measurements were made at two different combinations of polarization HH and VV, the first letter represents the polarization of the transmitting antenna and the second letter represents the polarization of receiving antenna (H and V stands for horizontal and vertical states of a horn antenna). Peak and average power sensor (E9327A, 50MHz to 18 GHz, -60 to 20 dBm) and EPM-P series power meter (E4416A, 9kHz to 110 GHz, -70 to 44 dBm) from Agilent Technologies were used to measure reflected power through paddy crop in a specular direction. The radar equation was used to compute σ^0 [146]. The experimental arrangement of the bi-spec scatterometer system is shown in Fig. 4.1 and Table 7.1 shows the specification of the bi-spec scatterometer system used in our study. The average value of three σ^0 measurements for each specular incidence angle and each polarization combination (HH and VV) at X and C band were reported at each day of measurement. The overall error in bistatic measurement was estimated by using the variation in the value of computed σ^0 to its mean value and was found between 0.05 to 0.20 dB.

7.2.3 Calibration

The bistatic specular system was calibrated using an adaption of the polarimetric bistatic calibration technique [147, 148]. A large flat aluminum plate was used as a calibration target for bistatic scattering measurement in specular direction on each day of observation. The bi-spec scatterometer system specification used for calibration was kept the same as the bistatic system used for paddy crop.

7.3 Statistical analysis

7.3.1 Support vector regression model

The support vector machine uses an algorithm to map non-linear problems into high dimensional feature space, developed by a Russian scientist [207]. The ε-SV regression algorithm starts with obtaining linear function as shown in Eq. 7.3 that maps all pair of input feature $x \in \mathbb{R}^m$ and observable $y \in \mathbb{R}$ in high dimensional feature space with ε precision simultaneously. It tries to reduce model complexity by minimizing $\frac{1}{2}||w||^2$ and introducing slack variable ξ_i, ξ_i^* that measures the variation of training sample outside ε-zone as shown in Eqs. 7.4 and 7.5 [208].

$$f(x_i, w) = < w, x_i > + b \tag{7.3}$$

$$Minimize \frac{1}{2}||w||^2 + C\sum_{i=0}^{n}(\xi_i + \xi_i^*) \tag{7.4}$$

$$\text{Subject to} \begin{cases} y_i - < w, x_i > - b \leq \varepsilon + \xi_i \\ < w, x_i > + b - y_i \leq \varepsilon + \xi_i^* \\ \xi_i, \xi_i^* \geq 0 \end{cases} \tag{7.5}$$

Where $<,>$ represent dot product and C and ε are hyperparameters of the SVR model. Further, solving a dual optimization problem that includes minimization of the Langrage function made of the objective function and corresponding constraints will provide key to reformulate Eq. 7.3 (detailed in [209, 210]).

$$f(x) = \sum_{i=0}^{n}(\alpha_i - \alpha_i^*) < x_i, x > + b \tag{7.6}$$

Where $w = \sum_{i=0}^{n}(\alpha_i - \alpha_i^*)x_i$, which can completely describe as a linear combination of the training pattern (x_i) called as a regressor. b stands for bias and α_i, α_i^* are Langrage multipliers.

Eq. 7.6 shows that support vector expansion depends on the mapping between training patterns x_i. Likewise, the mapping of support vector expansion can be written in an implicit way via kernels as shown in Eq. 7.7 [211].

$$f(x) = \sum_{i=0}^{n}(\alpha_i - \alpha_i^*)k(x_i, x) + b \tag{7.7}$$

The difference between Eqs. 7.6 and 7.7 indicates that w is no longer given explicitly. This paper compares the estimation of vegetation parameters from the remotely sensed microwave scattering response of paddy crop in specular direction using the SVR algorithm by choosing linear, polynomial and radial kernels.

7.3.2 Validation check and evaluation of the performance

The SVR algorithm solves the non-linear model regression approach by introducing a kernel trick. In this study, the SVR model using three different kernels namely linear, polynomial and radial were trained or tested on the computed specular bistatic scattering coefficient with a vegetation parameter as a response variable. Hyper-parameter C and ε and kernel parameter gamma were optimized using a 10-fold cross-validation method. The best combination of C and ε was selected according to the least centered root mean squared error. The model performance was evaluated by the difference between two patterns quantified in terms of their centered root mean square error $(CRMSE)$, correlation coefficient (R) and amplitude of their variations represented by the standard deviation (SD) of estimated (σ_f) and observed/reference data (σ_r) [212]. For an estimated (f) and observed/reference data(O), the formula for computing statistical parameters are shown in

Table 7.2. The overall mean of the data is indicated by an overbar. The performance and

Table 7.2 The statistical parameters used to evaluate the performance indices of the developed SVR model.

Standard deviation of observed/reference data	$\frac{\sum_1^n (O_i - \bar{O})^2}{n}$
Standard deviation of estimated data	$\frac{\sum_1^n (f_i - \bar{f})^2}{n}$
Correlation coefficient	$\frac{\sum_1^n (O_i - \bar{O})^2 (f_i - \bar{f})^2}{n\sigma_f \sigma_r}$
Centered root mean sqaure error	$\sqrt{\frac{\sum_1^n [(O_i - \bar{O}) - (f_i - \bar{f})]^2}{n}}$

robustness of the developed model were evaluated by the derived statistical parameters. These statistical parameters were summarized in the form of Taylor plot which provides an understanding of how well the model estimated data matches the observed/reference data.

7.4 Results and discussion

7.4.1 Analysis of bi-spec scattering response and optimal parameters selection

Figure 7.1 shows the temporal variation of vegetation growth parameters for the trans-planted paddy observed during in-situ measurements. The range of measured values of LAI, PH, FBm and VWC for the paddy crop during the entire set of observation were found to be (0.7374 - 4.8967) m^2m^{-2}, (0.4112 - 0.9522) m, (0.0896 - 2.6953) kgm^{-2} and (0.0710 - 1.9324) kgm^{-2}, respectively. An increasing trend for all vegetation parameters with the age was reported until the reproductive stage was achieved (i.e., till 292, DoY 2018). After the reproductive stage (grain filling and maturity stage), vegetation growth parameters started decreasing slightly due to a decrease in the moisture content of paddy crop. The

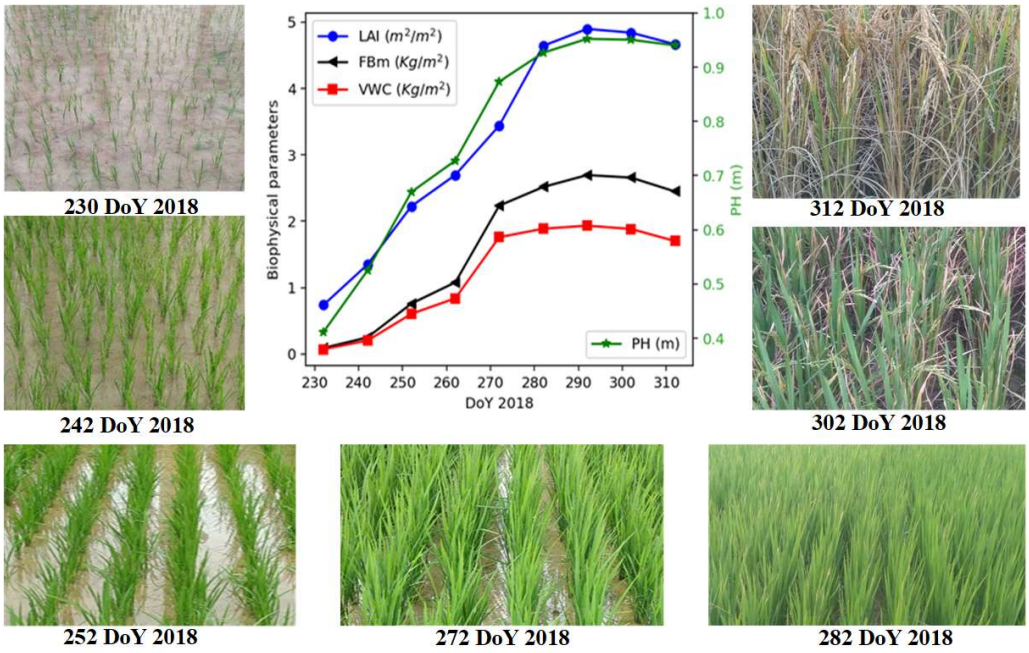

Fig. 7.1 The temporal variation of vegetation growth parameters of the transplanted paddy field during in-situ measurements.

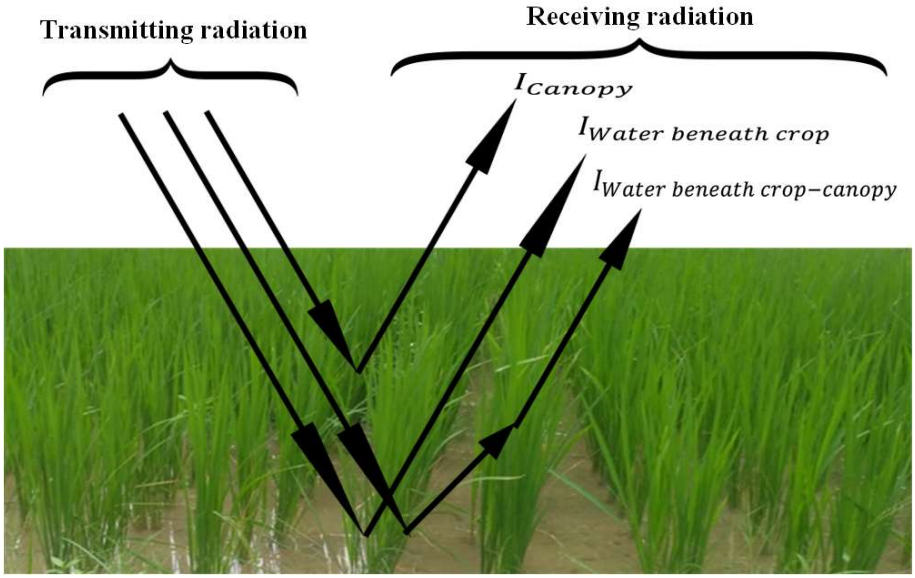

Fig. 7.2 Visualization of major coherent scattering components for the bistatic case..

Figures 7.3 and 7.4 show the temporal and angular variation of computed σ^0 at X and C bands for HH and VV polarizations. Figures 7.3 and 7.4 indicate that the temporal curve of σ^0 is sensitive to all stages of paddy crop and is dependent on the penetration power of

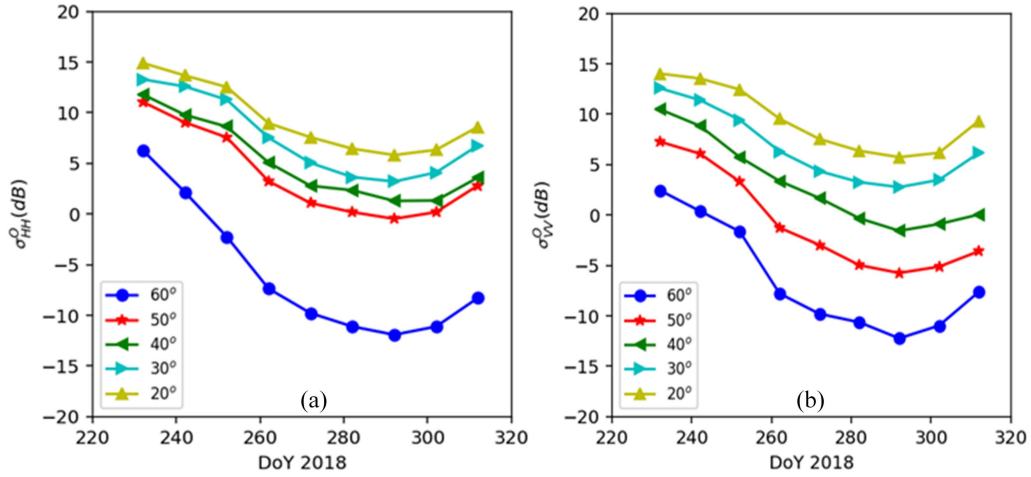

Fig. 7.3 Temporal pattern of σ^0 at a various specular angle of incidence ranging from 20° to 60° for X band (a) HH polarization (b) VV polarization.

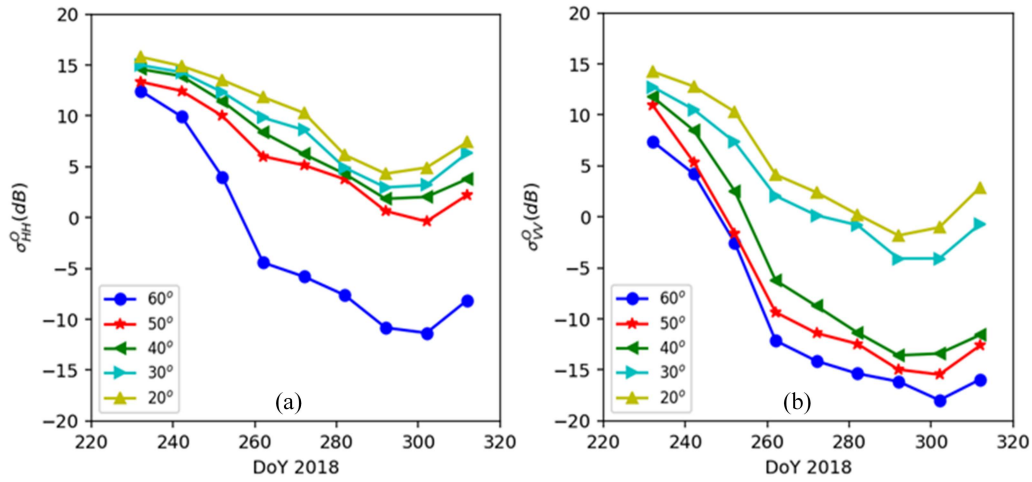

Fig. 7.4 Temporal pattern of σ^0 at a various specular angle of incidence ranging from 20° to 60° for C band (a) HH polarization (b) VV polarization.

microwave frequencies into paddy crop canopy. The sensitivity of the temporal curve of σ^0 was investigated by observing significant change in σ^0 with the temporal change in vegetation growth parameters of paddy crop. The dependency of the angular sensitivity of microwave (i.e., the temporal behavior of σ^0 over wide angular range varying from 20° to 60°) for bi-spec configuration and dominance of different types of scattering component contributing to σ^0 is based on the penetration power of microwave frequencies which has been taken into account in the present approach. The purpose of computing σ^0 is to

provide insight into polarimetric (HH/VV polarization) aspects of change in the coherent component and the incoherent component at X and C bands from a paddy crop observed from a down looking platform at an altitude of 3m in the specular direction. The σ^0 was found higher at HH polarization than VV polarization for both X and C bands. This may be due to the significant interaction of vertically polarized microwave frequencies with the vertical stalk which acts as a vertically oriented lossy dielectric cylinders at VV polarization. The decreasing trend of σ^0 with the age was reported till the reproductive stage (i.e., till 292, DoY 2018) of paddy crop. After reproductive stage (in grain filling and maturity stage), a slight increase in σ^0 was reported at X and C bands for both the polarization. The decreasing behavior of σ^0 is mainly due to attenuation of the coherent component by increasing growth parameters of the paddy crop overlaying the soil surface till reproductive stage. The coherent component is the main contribution to the value of σ^0 which include specular scattering from the soil beneath vegetation. Whereas the incoherent component was introduced by the temporal change in crop canopy geometry and vegetation growth parameters of the paddy crop. The significant interaction of microwave with the crop canopy medium and scattering of microwave frequencies other than specular direction due to crop canopy geometry reduces the microwave reflected/scattered power to the receiving antenna placed in the specular direction which leads to decrease in σ^0 till the growing stage of the paddy crop. After the reproductive stage, an incoherent component introduced by vegetation growth parameters started to decrease due to defoliation of emerging leaves after seed fill, an inclination of PH and decrease in vegetation moisture content which caused microwave to reach the soil beneath vegetation and led to enhance the value of σ^0 by the soil surface [116].

The dominance of scattering for a bi-spec configuration can be understood by integrating major scattering components into account. The value of σ^0 may include the scattering component due to the direct ground (in this case water beneath paddy crop), direct canopy

(volume interaction) and water beneath crop-canopy interaction based on the penetrating power of microwave frequencies as shown in Figure 7.2. The scattering due to direct water beneath crop in specular direction is the strongest among all the scattering components since water beneath crop acts as a smooth surface and gives a mirror-like reflection in the specular direction.

The values of σ^0_{HH} at C band were observed to be higher at HH-polarization as compared to σ^0_{HH} at X band for all specular incidence angles as shown in Figures 7.3(a) and 7.4(a). The reason behind the high value of σ^0_{HH} at C band is its higher penetrating ability than the X band. Due to the higher penetrating power, the value of σ^0_{HH} at C band might include the contribution from the water beneath crop and water beneath crop-canopy interaction as a dominant scattering component. Whereas, the dominant scattering component of σ^0_{HH} at X band might be dominated by water beneath crop interaction till leaf elongation stage (i.e. till 242, DoY 2018) of the paddy crop. After the leaf elongation stage, due to the lower penetrating power of X band, the value of σ^0_{HH} was dominated by only the direct canopy scattering component. In addition to that, for VV polarization, the values of σ^0_{VV} at C band were reported lower as compared to σ^0_{VV} at X band after the leaf elongation stage of paddy crop as shown in Figures 7.3(b) and 7.4(b). After the leaf elongation stages, an increase in vegetation growth parameters caused the significant interaction of vertically polarized microwave radiation with the vertical stalk which acts as vertically oriented lossy dielectric cylinders [213]. Due to the higher penetrating power of C band with respect to X band, the vertically polarized microwave can penetrate till water beneath crop which led to high attenuation by the vertically oriented stalks of the paddy crop. This resulted to decrease in the direct water beneath crop scattering component and the value of σ^0_{VV} at C band was dominated by water beneath crop- canopy scattering component. Whereas, due to lower penetrating ability of X band, vertically polarized microwave was unable to reach directly water beneath paddy crop and the value of σ^0_{VV}

at X band gets dominated by the direct canopy scattering component. Since, the direct canopy scattering component found stronger than the water beneath crop-canopy scattering component led to a higher value of σ^0_{VV} at X band as compared to σ^0_{VV} at C band.

The angular sensitivity for the temporal pattern of σ^0 can also be studied in terms of flatness/steepness of the curves. For X band, the temporal patterns of σ^0_{HH} and σ^0_{VV} were found flatter at 20°, 30°, 40°, 50° and steeper at 60°. For C band, the temporal pattern of σ^0_{HH} was found flatter at 20°, 30°,40°, 50° and steeper at 60°, whereas, the temporal pattern of σ^0_{VV} was found flatter at 20°, 30° and steeper at 40°, 50°, 60°. The angular behaviors of σ^0_{HH} and σ^0_{VV} at both X and C bands highly depends on the screening effect to the water beneath crop contribution due to the slant path in the paddy crop canopy [214]. At 20°, 30°,40° and 50° angle of incidence, no significant difference was observed in the temporal curve of the σ^0_{HH} and σ^0_{VV} at X band. Since, the temporal patterns of the σ^0_{HH} and σ^0_{VV} at X band is mainly contributed by the direct canopy scattering component (due to weak penetrating ability). The larger slant path in the paddy crop canopy at 60°, with respect to 20°, 30°,40° and 50°, caused to decrease the direct canopy scattering component which led to the steepness of the temporal curve for the σ^0_{HH} and σ^0_{VV} at X band. The similar response was observed for the temporal pattern of σ^0_{HH} at C band. However, the water beneath crop scattering component contributing to the value of σ^0_{HH} got weakened due to larger slant path at 60° led to the steepness of the temporal curve with respect to 20°, 30°,40° and 50°. In addition to that, the steepness of σ^0_{VV} for C band at 40°, 50°,60° with respect to 20°, 30° angle of incidence might be due to attenuation provided by the significant interaction of vertically polarized microwave frequencies with the vertical stalk available in larger slant path.

Correlation analysis was done between σ^0 and vegetation growth parameters to determine the optimum parameters of the bistatic system as summarized in Tables 7.3 and 7.4. The analysis shows a high correlation between σ^0 and vegetation growth parameters

Table 7.3 The correlation coefficient between the value of σ^0 and vegetation parameters at X band

Incidence angle (°)	The correlation coefficient between the σ^0 and vegetation parameters HH				VV			
	LAI	PH	FBm	VWC	LAI	PH	FBm	VWC
20	-0.943	-0.956	-0.961	-0.962	-0.926	-0.931	-0.949	-0.958
30	-0.937	-0.946	-0.959	-0.969	-0.934	-0.953	-0.949	-0.961
40	**-0.956**	**-0.974**	**-0.968**	**-0.972**	**-0.987**	**-0.992**	**-0.976**	**-0.973**
50	-0.937	-0.959	-0.951	-0.962	-0.970	-0.979	-0.971	-0.973
60	-0.939	-0.972	-0.939	-0.949	-0.928	-0.949	-0.941	-0.951

Table 7.4 The correlation coefficient between the value of σ^0 and vegetation parameters at C band

Incidence angle (°)	The correlation coefficient between the σ^0 and vegetation parameters HH				VV			
	LAI	PH	FBm	VWC	LAI	PH	FBm	VWC
20	-0.980	-0.938	-0.962	-0.945	-0.956	-0.960	-0.959	-0.961
30	-0.980	-0.949	-0.965	-0.952	-0.967	-0.975	-0.964	-0.961
40	**-0.988**	**-0.974**	**-0.982**	**-0.975**	**-0.970**	**-0.974**	**-0.964**	**-0.963**
50	-0.972	-0.970	-0.959	-0.944	-0.950	-0.980	-0.940	-0.943
60	-0.963	-0.960	-0.955	-0.953	-0.948	-0.975	-0.944	-0.947

at VV polarization as compared to HH polarization for X band at 40° angle of incidence. Whereas, the high correlation was found at HH polarization in comparison to VV polarization for C band at 40° angle of incidence. Therefore, HH polarization of C band at 40° angle of incidence and VV polarization of X band at 40° angle of incidence was chosen as an optimum parameter of the bi-spec scatterometer system. In particular, the highest correlation for LAI, FBm, and VWC were found at HH polarization for C band at 40° angle of incidence. Whereas, the highest correlation for PH was reported at VV polarization for X band at 40° angle of incidence. Based on correlation analysis, we concluded that σ^0 was more sensitive to LAI, FBm, and VWC at C band for HH polarization and PH at X band for VV polarization at 40° angle of incidence.

7.4.2 Input data, output data, and training/testing samples

The bi-spec scatterometer measurements were carried out at various phenological stages of paddy crop starting from 232, DoY 2018 to 312, DoY 2018 at the interval of 10 days for computing σ^0 along with measurements of vegetation growth parameters at each date of scatterometer measurement. Further, linear regression analysis was carried out to obtain the continuous data sets of σ^0 (σ^0_{VV} for X band and σ^0_{HH} for C band at 40° angle of incidence) and vegetation growth parameters on a daily basis to develop the SVR model for the retrieval of vegetation growth parameters. Out of total 81 data sets derived, 70% of the total datasets were selected to build a regression model called as training data set and 30% of data sets were used to check the accuracy of the built regression model called validation/testing data. To cover the variability of vegetation parameters for full paddy crop cycle, testing data were selected by regular sampling at the interval of 2 or 3 days.

7.4.3 Inversion result

Table 7.5 Optimized parameters of support vector regression model using linear, polynomial and radial kernel for vegetation parameter estimation at X_VV_40

Vegetation parameters	Kernels	Optimized parameter of SVR model (ε, C, γ, and d)	Number of support vectors
LAI	Linear	ε=0.1;C=28	31
	Polynomial	ε=0.3;C=2; d=3	41
	Radial	ε=0.1;C=6; γ=1	5
PH	Linear	ε=0.1;C=2	21
	Polynomial	ε=0.3;C=2; d=3	33
	Radial	ε=0.1;C=4; γ=1	6
FBm	Linear	ε=0.1;C=16	28
	Polynomial	ε=0.4;C=2; d=3	33
	Radial	ε=0.1;C=40; γ=1	7
VWC	Linear	ε=0.1;C=100	30
	Polynomial	ε=0.3;C=24; d=3	36
	Radial	ε=0.1;C=100; γ=1	10

Table 7.6 Optimized parameters of support vector regression model using linear, polynomial and radial kernel for vegetation parameter estimation at *C_HH_*40

Vegetation parameters	Kernels	Optimized parameter of SVR model (ε, C, γ, and d)	Number of support vectors
LAI	Linear	ε=0.1;C=4	30
	Polynomial	ε=0.1;C=100; d=3	43
	Radial	ε=0.1;C=8; γ=1	6
PH	Linear	ε=0.2;C=100	22
	Polynomial	ε=0.2;C=100; d=3	34
	Radial	ε=0.1;C=32; γ=1	5
FBm	Linear	ε=0.2;C=14	17
	Polynomial	ε=0.2;C=100; d=3	37
	Radial	ε=0.1;C=12; γ=1	14
VWC	Linear	ε=0.2;C=2	21
	Polynomial	ε=0.3;C=100; d=3	30
	Radial	ε=0.1;C=74; γ=1	7

Vegetation growth parameter retrieval was performed on testing data after completing the training of the SVR model via three different kernels i.e., linear kernel, polynomial kernel, and radial kernel. It was a highly nonlinear mapping of training data onto high dimensional feature space during inversion of the data sets consisting of σ^0_{VV} and σ^0_{HH} at 40° incidence angle for X and C bands, respectively. The performance of the SVR model was examined using a different kernel for the retrieval of vegetation growth parameters of paddy crop. This chapter mainly focuses on optimizing the following two hyperparameters and two kernel parameters. The first one is the thickness of the tube called epsilon (ε) which does not penalize errors below $\varepsilon \geq 0$. The second one is a cost (C) which penalizes any deviation outside the epsilon tube for the regularization of the regression network. The third and fourth are kernel parameters i.e. gamma (γ) and degree (d). The hyperparameters and kernel parameters are optimized using training datasets so that the cross-validation error is minimized. Tables 7.5 and 7.5 illustrate an optimized combination of hyperparameters and kernel parameters for the SVR model using linear, polynomial and radial kernels at the optimum parameters of bistatic configuration. Further, the optimum parameters of the

bistatic configuration are denoted by Band_Combination of HH/VV polrization_Incidence angle.

In this section, the performances of the developed SVR models using linear, polynomial and radial kernels for the vegetation growth parameter retrieval were evaluated at the optimum parameters of bi-spec scatterometer for both X and C bands. Figures 7.5(a)-7.8(a) show the comparison of the estimated values by the SVR model with the In-situ vegetation growth parameters. Figures 7.5(b)-7.8(b) show Taylor plots for the comparison of performance indices of SVR models using linear, polynomial and radial kernel between In-situ vegetation growth parameters (as reference) and estimated vegetation parameters at X_VV_40 and C_HH_40 by the SVR model. The performance indices of the SVR model using radial kernel at C_HH_40 shows best estimation for LAI, FBm and VWC as shown in Figures 7.5(b), 7.7(b), and 7.8(b). Whereas, the performance indices of the SVR model using radial kernel at X_VV_40 shows best result for PH estimation as shown in Figure 7.6(b). The estimation of LAI, PH, FBm and VWC by the SVR model using the radial kernel at C_HH_40 was found close to the in-situ observations with CRMSE = 0.0865 m^2m^{-2}, 0.0141 m, 0.0696 kgm^{-2} and 0.0605 kgm^{-2}, respectively. Although, the error estimates of SVR model using the radial kernel at X_HH_40 were found comparatively higher for LAI, FBm, VWC estimation with CRMSE =0.1188 m^2m^{-2}, 0.0889 kgm^{-2} and 0.0710 kgm^{-2}, whereas, it was found relatively lower for the PH estimation with CRMSE =0.0112 m. Also, the SD of LAI, FBm and VWC estimation were found closed to the SD of in-situ observation for the SVR model using radial kernel at C_HH_40 with SD = 1.4155, 0.9510 and 0.6800, respectively. While, the SD of PH estimation was found closed to the SD of in-situ observation for the SVR model using radial kernel at X_VV_40 with SD =0.1773. The values of R between in-situ data and estimated vegetation growth parameters by the SVR model using radial kernel at C_HH_40 were found to be 0.16%, 0.10%, 0.15% higher as compared to X_VV_40 for LAI, FBm, VWC, respectively.

Whereas, the value of R between the in-situ PH and estimated PH by the SVR model using radial kernel was found to be 0.1% lower at C_HH_40 as compared to X_VV_40. The results of analysis indicate best performance of the developed SVR model using radial kernel for the estimation of vegetation growth parameters of paddy crop followed by the SVR model using linear and polynomial kernels at C_HH_40 and X_VV_40 of the bi-spec configuration. Interestingly, the values of σ^0 having high correlation with the vegetation growth parameters of the paddy crop was found best for the retrieval of vegetation growth parameters by the developed SVR model using radial kernel. Thus, the estimation by the developed SVR model using radial kernel is preferred for LAI, FBm, and VWC at C band (C_HH_40), whereas the estimation of PH by the same developed SVR model is preferred at X band (X_VV_40) of the bi-spec configuration.

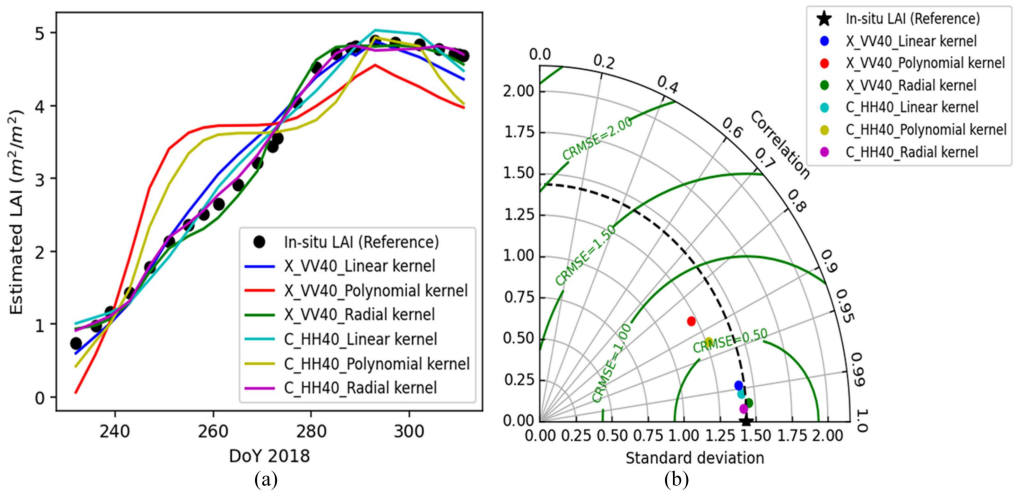

Fig. 7.5 (a) Estimated values of LAI by the SVR model using different kernels and in-situ LAI for paddy crop at X and C bands, and (b) Visualization of error estimates for LAI estimation by the Taylor plot.

7.5 Conclusion

The microwave scattering responses of vegetation growth parameters for paddy crop have been investigated by an indigenously designed dual-polarized (HH/VV) bi-spec

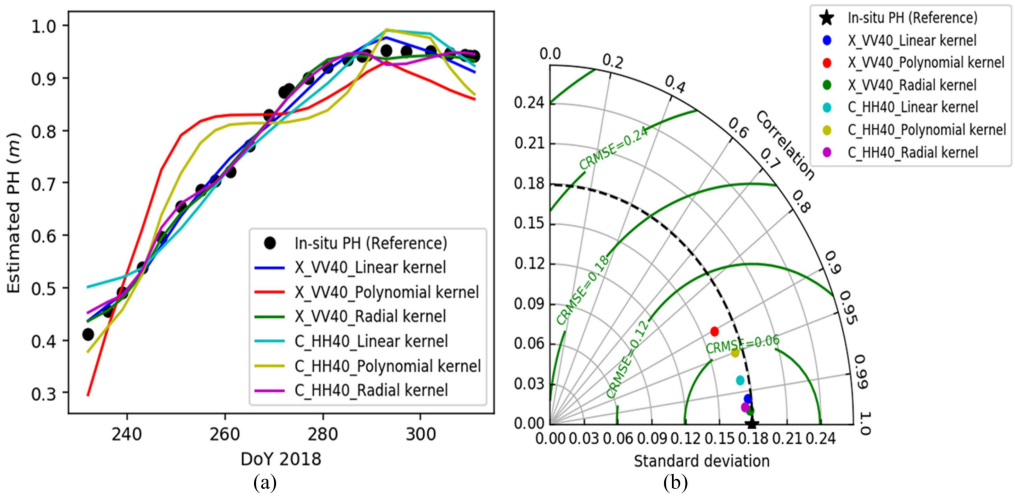

Fig. 7.6 (a) Estimated value of PH by the SVR model using different kernels and in-situ PH for paddy crop at X and C band, and (b) Visualization of error estimates for PH estimation by the Taylor plot.

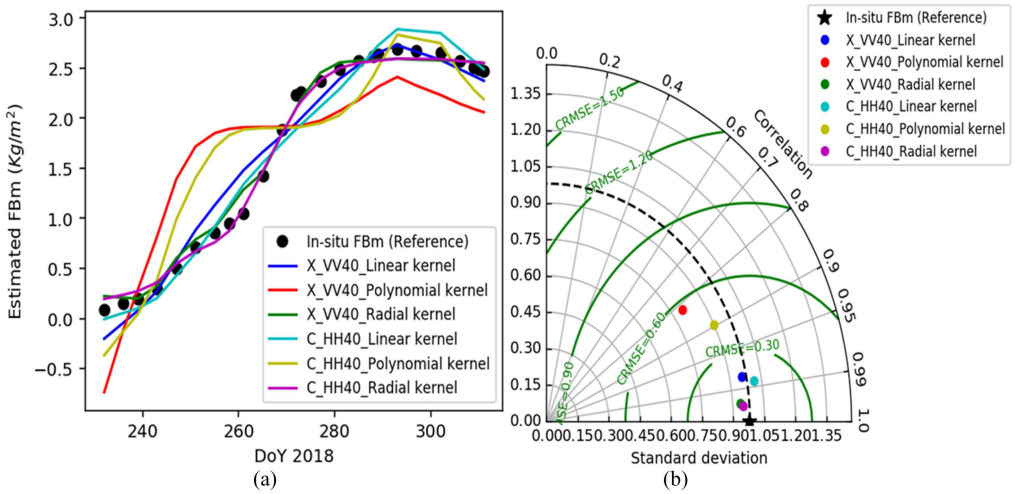

Fig. 7.7 (a) Estimated values of FBm by the SVR model using different kernels and in-situ FBm for paddy crop at X and C bands and (b) Visualization of error estimates for FBm estimation using the Taylor plot.

scatterometer system at X and C bands in the angular range of incidence angle 20° to 60° at the interval of 10°. The temporal variation of computed σ^0 were observed to decrease due to an increase in the vegetation growth parameters till maturity. After the maturity stage, σ^0 were found to increase slightly due to a decrease in the vegetation growth parameters. The temporal curve of σ^0 were observed to decreases with the increase in specular incidence

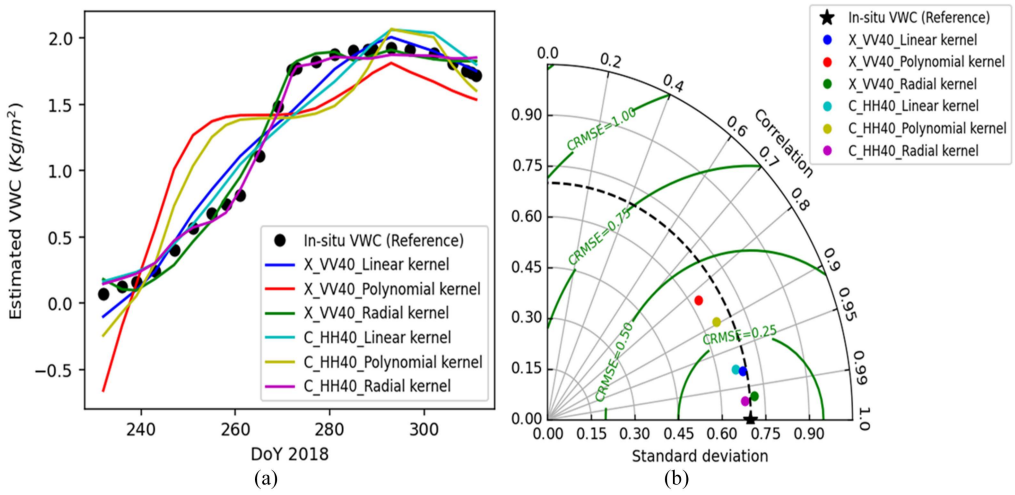

Fig. 7.8 (a) Estimated values of VWC by the SVR model using different kernels and in-situ VWC for paddy crop at X and C bands and (b) Visualization of error estimates for VWC estimation using the Taylor plot.

angle due to attenuation occurred in the dominant scattering component by the larger slant path of microwave in the paddy crop canopy.

Results of the correlation between σ^0 and vegetation growth parameters of paddy crop to find the optimum parameters of the bi-spec scatterometer system showed a higher correlation for LAI, FBm, and VWC at HH polarization, 40° angle of incidence at C band of Bi-spec scatterometer system in comparison to X band. Whereas, the higher correlation for PH with σ^0 was reported at VV-polarization, 40° angle of incidence at X band.

The potential of the developed SVR model with three different kernels (i.e linear, polynomial and radial) was evaluated for the estimation of vegetation growth parameters of paddy crop using the data collected by indigenously designed optimized bi-spec scatterometer system at X and C bands. The results of developed SVR model using radial kernel for the calibration and validation provided low values of CRMSE and SD indicating high correlations between the estimated values with the in-situ observation for LAI, FBm and VWC using *C_HH_*40. Based on the correlation analysis shown in Tables 7.3 and 7.4 and comparative analysis of the computed quantifiers such as CRMSE, SD and R between the estimated values of vegetation growth parameters by the SVR model using radial kernel

and in-situ observation shown in Figures 7.5(b)-7.8(b), the C band at HH polarization was found more sensitive for the monitoring of LAI, FBm, and VWC at 40° angle of incidence. While, the SVR model using radial kernel was found best for the estimation of PH by the developed SVR model using X_HH_40 followed by the SVR model using linear and polynomial kernels using bi-spec scatterometer data. Therefore, the results of the present study can be used as a reference for future advancement in the bistatic radar system for the monitoring of paddy crop more authentically ever before.

****